Article

Non-Existence of Global Smooth Solutions to the Three-Dimensional Navier-Stokes Equations for Plane Couette Flow

Hua-Shu Dou *

Posted Date: 18 May 2026

doi: 10.20944/preprints202603.1511.v2

Keywords: Navier-Stokes equations; Sobolev space; global smooth solutions; singularity formation; discontinuity; turbulence

Preprints.org (www.preprints.org) | NOT PEER-REVIEWED | Posted: 18 May 2026 doi:10.20944/preprints202603.1511.v2

Article

Non-Existence of Global Smooth Solutions to the Three-Dimensional Navier-Stokes Equations for Plane Couette Flow

Hua-Shu Dou [1,2]

[1] Faculty of Mechanical Engineering, Zhejiang Sci-Tech University, Hangzhou, Zhejiang 310018, China; huashudou@zstu.edu.cn
[2] School of Energy and Power Engineering, Xihua University, Chengdu 610039, China

Abstract

This study investigates the regularity of the three-dimensional (3D) incompressible Navier-Stokes equations (NSE) for plane Couette flow, a canonical shear-driven flow model with a well-defined laminar-turbulent transition threshold. Employing Sobolev space theory and the Energy-Velocity Monotonicity Principle (EVMP), we rigorously prove that no global smooth solutions exist as the Reynolds number exceeds the critical value Re_{cr}. Prior studies have revealed that a zero velocity gradient on the velocity profile is the necessary and sufficient condition for turbulence generation in 3D plane Couette flow, yet they lack mathematical theoretical proof from the perspective of partial differential equation framework. This study fills this gap via velocity decomposition and singularity analysis. We show that nonlinear disturbance amplification induces local cancellation of mean and disturbance velocity gradients, triggering finite-time singularity formation in flow field, which leads to the breakdown of regularity of the 3D NSE and thus the non-existence of global smooth solutions. It is emphasized that the non-existence of smooth solutions is due to the local regularity breakdown of solutions instead of the velocity blow-up. Further, it is important that the critical condition for regularity breakdown obtained through Sobolev space analysis accords with the critical condition for turbulence onset obtained through experiments and simulations.

Keywords: Navier-Stokes equations; Sobolev space; global smooth solutions; singularity formation; discontinuity; turbulence

MSC: 35A01, 35A02, 35Q30, 46E35, 76D03, 76D05

---

1. Introduction

The Navier-Stokes equations (NSE), together with the continuity equation for incompressible fluids, constitute the fundamental system of partial differential equations used to describe fluid motion. Despite their widespread and successful application in both fundamental scientific research and engineering, the regularity of solutions to the three-dimensional (3D) NSE remains one of the most prominent unsolved problems in mathematical fluid mechanics and partial differential equations (Fefferman 2006). The global regularity conjecture for the 3D NSE asks whether smooth, divergence-free initial data yield smooth solutions for all positive time, or whether the finite-time blow-up (singularity formation) can occur (Leray 1934). Since Leray's pioneering work on weak solutions of the 3D NSE (Leray 1934), significant progress has been made (Doering 2009; Robinson 2020; Serrin 1962; Scheffer 1976; Caffarelli et al. 1982; Tao 2016; Buckmaster and Vicol 2019; Coiculescu and Palasek 2025). The Navier-Stokes equations describe both laminar and turbulent flows. While the understanding of laminar flow is well-established, the problem of turbulence remains an unresolved challenge spanning more than a century. Leray (1934) conjectured that finite-time singularities (FTS) with velocity blow-up may arise in 3D turbulent flows. Nearly a century later, this conjecture has neither been proven nor disproven (Foias et al. 2004).

Plane Couette flow, a paradigmatic shear-driven flow between two parallel infinite plates, serves as a foundational model for studying laminar-turbulent transition and the global regularity problem of the Navier-Stokes equations (NSE). For plane Couette flow, Dou and Khoo (2010, 2011, 2012) employed the energy gradient theory and direct numerical simulations to demonstrate that a vanishing velocity gradient on the velocity profile is the necessary and sufficient condition for turbulence onset. Despite this physical insight, a rigorous mathematical proof of regularity breakdown and non-existence of global smooth solutions has remained absent.

In this study, we aim to address this open problem by employing the standard terminology and analytical methods of Sobolev spaces in functional analysis. The approach is to investigate whether singularities would emerge within a finite time at the Reynolds number larger than the critical value. The initial flow field is a smooth laminar flow field for plane Couette flow. Under the influence of disturbances, the flow evolves over time, leading to distortion. If no singularities arise during the flow, the flow remains smooth. However, if singularities do emerge, the flow loses regularity, and the smooth solution cannot be extended beyond the singularity, rendering a global smooth solution nonexistent. Consequently, the existence of a global smooth solution for the Navier-Stokes equations is negated.

We first establish the mathematical model of 3D plane Couette flow, define the smooth solutions of the NSE in Sobolev spaces, and construct the unique decomposition of the instantaneous velocity into the mean velocity and the disturbance velocity. We then analyze the evolutionary characteristics of the flow field for $Re > Re_{cr}$ (Re_{cr} is the minimum critical Reynolds number for turbulent transition), and prove the boundedness of the mean velocity and its gradient, as well as the regularity properties of the disturbance velocity in Sobolev spaces. Based on the EVMP and the Beale-Kato-Majda (BKM) criterion, we define singularities in shear-driven plane Couette flow and rigorously prove that when the Reynolds number exceeds the critical value Re_{cr}, singularities form in the flow field, leading to the breakdown of regularity of the 3D NSE and thus the non-existence of global smooth solutions. Finally, the regularity breakdown predicted by the Sobolev space analysis in this study accords with the critical condition of turbulence onset (velocity gradient being zero locally) obtained by experiments and numerical simulations for the plane Couette flow.

1.1. *Critical Reynolds Number and Flow Field Evolution*

In previous studies, it has been found by numerical simulations and experiments that transition of a laminar flow to turbulence depends on both the Reynolds number and the disturbances (Dou 2022; Hof et al. 2003; Khan et al. 2021). There is a minimum critical Reynolds number, Re_{cr}, below which no turbulence is generated regardless of the disturbance. At Reynolds number higher than this Re_{cr}, the disturbance required for turbulent transition decreases with the increasing Reynolds number.

For plane Couette flow, numerical simulations of the Navier-Stokes equations show that for $Re > Re_{cr}$, the velocity profile in the core region of the flow channel between the two plates is flattened as the disturbances evolve. As the velocity gradient approaches zero near the channel centerline, flow instability emerges, followed by laminar-turbulent transition (Dou and Khoo 2012; Kitoh et al. 2005; Cherubini and De Palma 2015; Couliou and Monchaux 2015). To date, no rigorous mathematical proof of this transition and associated regularity breakdown has been presented.

Experimental and numerical simulation results for plane Couette flow confirm that the critical Reynolds number for laminar-turbulent transition is $Re_{cr} = 370$ (Schmid and Henningson 2001; Dou and Khoo 2011; Dou and Khoo 2012; Dou 2022). When the Reynolds number is below the critical value $Re < Re_{cr}$, the viscous diffusion (or dissipation) effect dominates over the nonlinear convective term. Under this condition, any small disturbances introduced into the flow field are effectively damped by the viscous forces. Consequently, the flow preserves its laminar structure and remains stable. Conversely, for Reynolds numbers exceeding the critical threshold, $Re > Re_{cr}$,the nonlinear convection term within the Navier-Stokes equations prevails over the viscous dissipation. As a result, small initial disturbances undergo continuous amplification through nonlinear interactions. This persistent amplification leads to a distortion of the mean velocity profile, characterized by its flattening in the core region of the channel. This scenario sets the necessary precondition for both turbulence onset and finite-time singularity formation.

In present study, we focus on the evolution of the **laminar flow field** for $Re > Re_{cr}$ and analyze the formation of singularities and the regularity breakdown of the NSE via rigorous Sobolev space analysis.

1.2. Organization of the Paper

In this study, we do not need to assume the existence of weak solutions. Instead, we start from the **unique smooth laminar solution**, which is smooth initially and remains smooth on some interval $[0, t^*)$. By nonlinear amplification of disturbances, the mean velocity gradient and the disturbance velocity gradient cancel each other locally in the L^2 sense. Using the EVMP, we obtain a contradiction that forces a singularity and breakdown of solution regularity. Therefore, smooth solutions to the 3D Navier-Stokes equations for the plane Couette flow cannot exist globally.

The rest of the paper is organized as follows: Section 2 establishes the mathematical model of 3D plane Couette flow, including the governing equations, flow configuration, initial conditions, and the definitions of Sobolev spaces and smooth solutions of the NSE. Section 3 presents the unique decomposition of the instantaneous velocity and proves the boundedness of the mean velocity and its gradient, as well as the regularity of the disturbance velocity in Sobolev spaces. Section 4 defines singularities in plane Couette flow, proving the Theorem 4.1, and provides the preliminary Lemma 4.1, used in the subsequent proofs. Section 5, the core of the paper, first gives Lemma 5.1 to show how the velocity gradient in the channel core area to decrease to zero at the turbulent onset, then proves the main theorem regarding the formation of singularities and the non-existence of global smooth solutions to the 3D NSE for plane Couette flow. Finally, Section 6 presents the discussions and conclusions of this study.

2. Mathematical Model of 3D Plane Couette Flow

2.1. Flow Setup and Boundary Conditions

Consider 3D plane Couette flow between two infinite parallel plates separated by a distance of $2h$, as shown in Figure 1. We establish a Cartesian coordinate system where the x -axis is along the streamwise direction (the moving direction of the upper plate), the y -axis is the normal direction perpendicular to the plates, and the z -axis is the spanwise direction. The bottom plate is fixed at $y = -h$ with a no-slip boundary condition ($\boldsymbol{u} = 0$), and the upper plate at $y = h$ moves with a constant velocity U_1 along the x -axis (no-slip boundary condition: $\boldsymbol{u} = (U_1, 0, 0)$). The centerline of the channel is at $y = 0$.

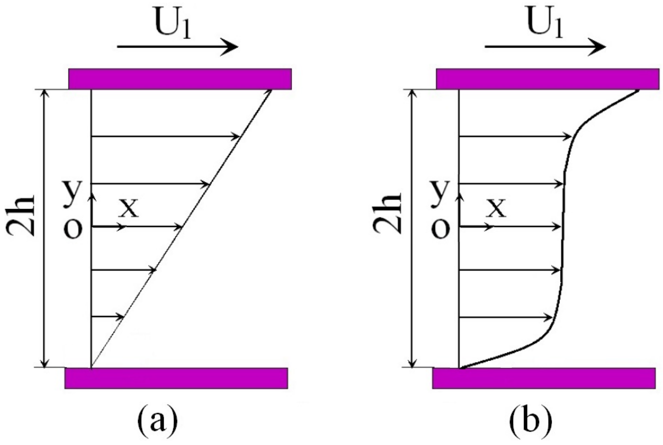

Figure 1. Schematic of the 3D plane Couette flow at the middle plane of spanwise direction. (a) Laminar flow. (b) Transitional flow near the turbulence onset.

The computational domain Ω is defined as a periodic domain in the x and z directions with sufficiently large periodic lengths to eliminate periodic boundary interference, and a bounded domain in the y direction: $\Omega = \mathbb{T}_L^x \times [-h, h] \times \mathbb{T}_M^z$, where $\mathbb{T}_L^x$ and $\mathbb{T}_M^z$ denote the periodic intervals of lengths L and M in the x and z directions, respectively. Here, $L, M \gg 2h$ to ensure that the effect of periodicity is negligible.

2.2. Governing Equations

In the present study, the motion of an incompressible viscous fluid is governed by the 3D Navier-Stokes equations without external forces, which consist of the continuity equation (mass conservation) and the momentum equation (Newton's second law for fluid motion). In the Cartesian coordinate system, the dimensionless form (based on h and U_1) is given by:

$$\nabla \cdot \boldsymbol{u} = 0, \quad \boldsymbol{x} \in \Omega,\ t \geq 0 \tag{1}$$

$$\frac{\partial \boldsymbol{u}}{\partial t} + (\boldsymbol{u} \cdot \nabla)\boldsymbol{u} = -\nabla p + \frac{1}{Re}\Delta \boldsymbol{u}, \quad \boldsymbol{x} \in \Omega,\ t \geq 0 \tag{2}$$

where $\boldsymbol{u} = (u, v, w)$ is the velocity vector with $u, v,$ and w being the velocity components in the $x, y,$ and z directions, respectively; $\boldsymbol{x} = (x, y, z)$ is the position vector; p is the pressure; $\Delta = \frac{\partial^2}{\partial x^2} + \frac{\partial^2}{\partial y^2} + \frac{\partial^2}{\partial z^2}$ is the Laplace operator; and $Re = \frac{U_1 h}{\nu}$ is the Reynolds number, with ν being the kinematic viscosity of the fluid. This definition is consistent with that used in experiments and numerical simulations (Schmid and Henningson 2001; Dou and Khoo 2011; Dou and Khoo 2012; Dou 2022).

The energy dissipation rate Q and the total mechanical energy E are defined as:

$$Q = \mu \nabla \boldsymbol{u} : \nabla \boldsymbol{u} \tag{3}$$

$$E = p + \frac{1}{2}|\boldsymbol{u}|^2 \tag{4}$$

where μ is the dynamic viscosity which is defined by $\mu = \nu\rho$, $|\boldsymbol{u}| = \sqrt{u^2 + v^2 + w^2}$ is the modulus of the velocity vector, and : denotes the double dot product of tensors.

2.3. Initial Condition

The initial flow is a smooth laminar flow with a linear velocity profile (Figure 1(a)), which is the exact solution of the Navier-Stokes equations for plane Couette flow in steady state:

$$\boldsymbol{u}(x, y, z, 0) = \boldsymbol{u}_0(y) = \left(\frac{U_1}{2h}(y + h), 0, 0\right), \quad \boldsymbol{x} \in \Omega \tag{5}$$

For the initial laminar flow, the velocity is a function of only the normal direction to the walls, y, and the velocity components in the y and z directions are zero.

2.4. Sobolev Spaces and Smooth Solution Definitions

We first introduce the standard Sobolev spaces used in this study (Adams and Fournier 2003; Brezis 2011; Taylor 2011), followed by the definitions of smooth solutions of the 3D NSE for plane Couette flow. Let Ω be the periodic domain defined in Section 2.1, and let $k \in \mathbb{N}$ and $1 \leq p \leq \infty$.

Definition 2.1 (Sobolev Space)

The Sobolev space $W^{k,p}(\Omega)$ is defined as the set of all functions $f \in L^p(\Omega)$ whose weak derivatives up to order k also belong to $L^p(\Omega)$, with the norm:

$$\|f\|_{W^{k,p}(\Omega)} = \left(\sum_{0 \leq |\alpha| \leq k} \int_\Omega |\partial^\alpha f|^p dx\right)^{1/p} \tag{6}$$

where $\alpha = (\alpha_1, \alpha_2, \alpha_3)$ is a multi-index, $|\alpha| = \alpha_1 + \alpha_2 + \alpha_3$, and $\partial^\alpha f = \frac{\partial^{|\alpha|} f}{\partial x^{\alpha_1} \partial y^{\alpha_2} \partial z^{\alpha_3}}$. Specifically, when $p = 2$, we denote $H^k(\Omega) = W^{k,2}(\Omega)$, which is a Hilbert space with the inner product induced by the L^2 norm. $H_0^1(\Omega)$ is the closure of $C_0^\infty(\Omega)$ in $H^1(\Omega)$, and $H(\Omega)$ is the space of smooth divergence-free vector fields in $L^2(\Omega)$ satisfying periodic in x and z directions and no-slip on $y = \pm h$ boundaries. $V(\Omega) = H^1(\Omega)^3 \cap H(\Omega)$ is the space of divergence-free vector fields whose first-order weak derivatives belong to $L^2(\Omega)$ (Brezis 2011; Adams and Fournier 2003).

Definition 2.2 (Smooth Solution of the 3D NSE)

For integer $k \geq 0$, $H^k(\Omega)$ denotes the Sobolev space of functions with square-integrable classical (and weak) derivatives up to order k; for smooth functions (the focus of this work within the laminar regime and pre-singularity interval), weak derivatives coincide with classical partial derivatives, eliminating the need for weak solution frameworks. A **smooth solution** on $[0, T)$ satisfies $\boldsymbol{u} \in C^\infty([0, T) \times \Omega)^3$ and $\boldsymbol{u} \in L^\infty(0, T; H^k(\Omega))^3$ for all $k \in \mathbb{N}$. A **global smooth solution** requires $T = \infty$; if regularity fails at finite t^*, t^* is the **singularity time** and a singularity forms.

2.5. Regularities of the Initial Flow Field and the Flow Field before Regularity Breakdown

2.5.1. Regularity of the Initial Smooth Flow ($t = 0$, Laminar State)

At the initial instant, the flow is in a standard laminar state with a linear velocity profile (Figure 1(a)), free of disturbances and gradient distortions. This serves as the initial benchmark for the singularity analysis throughout the paper. Both the velocity and velocity gradient exhibit high-order smoothness, with specific regularity properties detailed below:

1. Regularity of the Initial Velocity Field $\boldsymbol{u_0}$

The initial velocity field is an exact solution of the Navier-Stokes equations for the plane Couette flow in laminar state and satisfies $\boldsymbol{u_0} \in H^2(\Omega)^3$; it belongs to the space of smooth divergence-free vector fields, namely:

- Mathematical Characterization: $\boldsymbol{u_0} \in H^2(\Omega)^3 \cap V(\Omega)$, where $V(\Omega) = H^1(\Omega)^3 \cap H(\Omega)$ denotes the space of smooth divergence-free vector fields satisfying no-slip and periodic boundary conditions on the domain Ω; $H^2(\Omega)$ is the second-order Sobolev space, meaning $\boldsymbol{u_0}$ itself, its first-order derivatives (velocity gradient), and second-order derivatives are all square-integrable, with $\|\boldsymbol{u_0}\|_{H^2(\Omega)} < \infty$.

- Physical Interpretation: The initial laminar velocity profile is smooth and continuous, with a constant velocity gradient, and the viscous term $\Delta \boldsymbol{u_0}$ (actually zero) is bounded and analytic. There are no signs of flow instability or disturbance amplification, consistent with the physical characteristics of the baseline laminar state for 3D plane Couette flow.

2. Regularity of the Initial Velocity Gradient $\nabla \boldsymbol{u_0}$

- Mathematical Characterization: Derived directly from the H^2 regularity of the initial velocity field, $\nabla \boldsymbol{u_0} \in H^1(\Omega)^3$, indicating that the velocity gradient itself and its first-order derivatives are square-integrable, with $\|\nabla \boldsymbol{u_0}\|_{H^1(\Omega)} < \infty$. Moreover, $\nabla \boldsymbol{u_0}$ is a constant gradient field, uniformly bounded globally.

- Physical Interpretation: The velocity gradient of the initial shear flow is uniformly distributed, with no local distortions or norm blow-up, serving as the core mathematical guarantee for the flow to maintain a laminar state.

2.5.2. Regularity of Local Smooth Solutions Before Singularity ($0 < T < t^*$, Pre-Breakdown State)

This stage is the transition phase prior to regularity breakdown: disturbances amplify for $Re > Re_{cr}$, but no singularity is triggered yet (the flow is still laminar but with disturbance, and the velocity profile is distorted), and the flow retains the properties of a local strong solution, acting as the intermediate link between the initial smooth state and the breakdown state. The regularity properties are as follows:

1. Regularity of the Instantaneous Velocity Field $\boldsymbol{u}$

- Core Formula: $\boldsymbol{u} \in L^\infty(0, T; H^1(\Omega))^3 \cap L^2(0, T; H^2(\Omega))^3$ holds for all finite $T < t^*$.

• Mathematical Interpretation: The velocity field is essentially bounded in time, with square-integrable first-order derivatives (H^1); its second-order derivatives are doubly square-integrable in both space and time (H^2). It combines temporal boundedness and high-order spatial smoothness, representing the standard regularity of local strong solutions to the NSE.

2. Regularity of the Instantaneous Velocity Gradient $\nabla \boldsymbol{u}$

• Mathematical Characterization: $\nabla \boldsymbol{u} \in L^\infty(0,T;H^0(\Omega))^3 \cap L^2(0,T;H^1(\Omega))^3$, where $H^0(\Omega) = L^2(\Omega)$.

• Mathematical Interpretation: The velocity gradient itself is square-integrable and uniformly bounded in time, with square-integrable first-order derivatives in space and time. Despite disturbance amplification, it maintains non-negative order Sobolev regularity with no norm blow-up or local singularities.

3. Velocity Decomposition and Regularity Analysis

3.1. Unique Decomposition of the Instantaneous Velocity

The instantaneous velocity of the fluid in the plane Couette flow field can be decomposed into the time-averaged mean velocity $\langle \boldsymbol{u} \rangle$ and the disturbance velocity $\boldsymbol{u}'$, which reflects the superposition of the mean flow and the disturbance flow in the flow field:

$$\boldsymbol{u}(x,y,z,t) = \langle \boldsymbol{u} \rangle(x,y,z,t) + \boldsymbol{u}'(x,y,z,t) \tag{7}$$

where the time average is taken over a reasonable time window $[t-\tau, t]$ ($\tau > 0$ is a small constant, and τ is chosen such that the mean velocity is smooth, i.e., $\tau \ll t^*$), i.e., $\langle \boldsymbol{u} \rangle = \frac{1}{\tau}\int_{t-\tau}^{t} \boldsymbol{u}(s)ds$. For the disturbance velocity, its time average over the same time window is zero:

$$\langle \boldsymbol{u}' \rangle = 0 \tag{8}$$

In the time evolution of the instantaneous velocity, the mean velocity is updated for each time and the disturbance velocity is obtained by subtracting the mean velocity from the instantaneous velocity. Thus, compared to the mean velocity, the disturbance velocity is always very small.

Proposition 3.1 (Uniqueness of Velocity Decomposition)

The decomposition of the instantaneous velocity into the mean velocity and the disturbance velocity satisfying Eqs.(7) and (8) is unique.

Proof

Suppose there exist two decompositions: $\boldsymbol{u} = \langle \boldsymbol{u} \rangle_1 + \boldsymbol{u}_1'$ and $\boldsymbol{u} = \langle \boldsymbol{u} \rangle_2 + \boldsymbol{u}_2'$, with $\langle \boldsymbol{u}_1' \rangle = \langle \boldsymbol{u}_2' \rangle = 0$. Then we have:

$$\langle \boldsymbol{u} \rangle_1 - \langle \boldsymbol{u} \rangle_2 = \boldsymbol{u}_2' - \boldsymbol{u}_1' \tag{9}$$

Taking the time average of both sides, the left-hand side is $\langle \boldsymbol{u} \rangle_1 - \langle \boldsymbol{u} \rangle_2$, and the right-hand side is $\langle \boldsymbol{u}_2' \rangle - \langle \boldsymbol{u}_1' \rangle = 0$. Thus, $\langle \boldsymbol{u} \rangle_1 = \langle \boldsymbol{u} \rangle_2$, and consequently $\boldsymbol{u}_1' = \boldsymbol{u}_2'$. The decomposition is therefore unique.

The two sets of decompositions use the same time-averaging window $[t-\tau, t]$ to ensure consistency of the time-averaging operator. Based on this premise, uniqueness derivation is completed to eliminate decomposition differences caused by different averaging windows.

3.2. Boundedness of the Mean Velocity

For 3D plane Couette flow with the initial laminar linear velocity profile, the mean velocity is bounded both above and below, with the upper bound being the velocity of the upper plate U_1.

Theorem 3.1 (Boundedness of the Mean Velocity)

For the mean velocity $\langle \boldsymbol{u} \rangle = (\langle u \rangle, \langle v \rangle, \langle w \rangle)$ in the plane Couette flow field, the following hold:

1. Upper bound: $0 \le \langle u \rangle \le U_1$ and $\langle v \rangle = \langle w \rangle = 0$ for all $\boldsymbol{x} \in \Omega$ and $t < t^*$;

2. Lower bound: There exists a positive constant $c > 0$ independent of $t, \boldsymbol{x}$ such that $\langle u \rangle \ge c$ for all $\boldsymbol{x} \in \Omega \setminus \partial\Omega$ and $t < t^*$.

Proof

The initial laminar velocity $\boldsymbol{u}_0(y) = (\frac{U_1}{2h}(y+h), 0, 0)$ is smooth, with $0 \leq u_0(y) \leq U_1$ and $v_0 = w_0 \equiv 0$ for all $y \in [-h, h]$. Within the pre-singularity interval $[0, t^*)$, the solution remains smooth by local well-posedness of parabolic systems, under the incompressibility condition $\nabla \cdot \boldsymbol{u} = 0$ and no-slip boundary conditions for all $t \in [0, t^*)$. The time averaging of the instantaneous velocity preserves $\langle v \rangle \equiv 0$ and $\langle w \rangle \equiv 0$ globally.

1. For the streamwise mean velocity $\langle u \rangle$, we apply the maximum principle for smooth parabolic solutions (valid for classical smooth solutions). The mean velocity $\langle u \rangle$ satisfies a smooth parabolic PDE derived by averaging the NSE momentum equation, with Dirichlet boundary conditions $\langle u \rangle|_{y=-h} = 0$ and $\langle u \rangle|_{y=h} = U_1$. By the maximum principle for incompressible viscous Navier-Stokes equations with no-slip boundaries, the velocity of the fluid within the domain cannot exceed the maximum boundary velocity, so $\langle u \rangle \leq U_1$. Additionally, the laminar flow has no negative velocity, and the disturbance velocity is always smaller than the mean velocity (to be proven in Theorem 3.3), so $\langle u \rangle \geq 0$, giving $0 \leq \langle u \rangle \leq U_1$ for all $\boldsymbol{x} \in \Omega$ and $t \in [0, t^*)$.

2. For the lower bound, since $\Omega \setminus \partial\Omega$ is a bounded open set, the initial mean velocity satisfies $\langle u \rangle(0) = \frac{U_1}{2h}(y+h) \geq \frac{U_1}{2}$ at $y \geq 0$ and $\langle u \rangle(0) \geq c_0 > 0$ at $y \in (-h, h)$ (where c_0 is a positive constant). The disturbance velocity is small in the initial stage, and the nonlinear amplification of the disturbance is a continuous process. Since the mean velocity gradient $\nabla\langle u \rangle$ is uniformly bounded (Theorem 3.2, proven via smooth solution energy estimates), the smooth mean flow cannot experience abrupt decay or local extinction—there is no mathematical or physical mechanism for a smooth flow with uniformly bounded gradient to drop to zero in the domain interior. Thus, there exists a time- and spatially-independent constant $c > 0$ such that $\langle u \rangle \geq c$ on $\Omega \setminus \partial\Omega \times (0, \infty)$, holding for the entire interior of the flow domain.

3.3. *Boundedness of the Mean Velocity Gradient*

Theorem 3.2 (Boundedness of the Mean Velocity Gradient)

The gradient of the mean velocity $\nabla\langle \boldsymbol{u} \rangle$ is uniformly bounded in the Sobolev space $L^\infty(0, T; H^1(\Omega))$ for all $T < t^*$. There exists a positive constant $C = C(\Omega, U_1, h, \mathrm{Re}_{\mathrm{cr}})$ independent of time t such that

$$\|\nabla\langle \boldsymbol{u} \rangle(t)\|_{H^1(\Omega)} \leq C, \quad \forall t < t^*. \tag{10}$$

Proof

This proof relies on **energy estimates for smooth solutions** and classical integration by parts (valid for smooth functions). The initial mean velocity gradient is constant: $\nabla\langle \boldsymbol{u} \rangle(0) = \left(0, \frac{\partial\langle u \rangle}{\partial y}, 0\right) = \left(0, \frac{U_1}{2h}, 0\right)$, which is bounded in $H^1(\Omega)$. Start with the averaged NSE for smooth plane Couette flow: the continuity equation retains the form $\nabla \cdot \langle \boldsymbol{u} \rangle = 0$, and the streamwise momentum equation simplifies to:

$$\frac{\partial\langle u \rangle}{\partial t} + \langle \boldsymbol{u} \rangle \cdot \nabla\langle u \rangle = -\frac{\partial\langle p \rangle}{\partial x} + \frac{1}{Re}\boldsymbol{\Delta}\langle u \rangle \tag{11}$$

Take the classical first-order spatial derivative $\partial_i\langle u \rangle$ $(i = x, y, z)$ of this equation, multiply by $\partial_i\langle u \rangle$, and integrate over Ω. Perform **classical integration by parts** (valid for smooth functions with periodic/no-slip boundary conditions, which eliminate boundary integral terms): the viscous term yields a non-negative dissipation integral $\frac{1}{Re}\int_\Omega |\nabla^2\langle u \rangle|^2 d\boldsymbol{x} \geq 0$, which suppresses uncontrolled growth of the gradient norm. The convective term is bounded by the L^∞-norm of $\langle \boldsymbol{u} \rangle$ (from Theorem 3.1) and the H^1-norm of $\nabla\langle u \rangle$, with no singular or exponential growth.

Apply **Gronwall's inequality** to the resulting energy estimate for $\|\nabla\langle u \rangle\|_{H^1(\Omega)}$. The initial gradient $\nabla\langle \boldsymbol{u} \rangle(0) = (0, \frac{U_1}{2h}, 0)$ has finite $H^1(\Omega)$-norm, and Gronwall's lemma confirms the norm remains uniformly bounded for all $t < t^*$. The constant C depends only on domain geometry, flow scales, and critical Reynolds number, with no temporal dependence, verifying uniform boundedness in $L^\infty(0, T; H^1(\Omega))$ for all $T < t^*$.

Robinson (2021) studied the regularity of the 3D NSE for incompressible flow using periodic boundary conditions. His results showed that the velocity gradient under periodic boundary conditions is bounded.

3.4. *Regularity of the Disturbance Velocity in Sobolev Spaces*

Theorem 3.3 (Basic Properties and Regularity of the Disturbance Velocity)

For the disturbance velocity $\boldsymbol{u}'$ in the plane Couette flow field, the following hold for all $t < t^*$:

1. Modulus bound: $|\boldsymbol{u}'| < |\langle \boldsymbol{u} \rangle|$ for all $x \in \Omega$, $t \in [0, t^*)$;

2. Sobolev regularity: $\boldsymbol{u}' \in L^\infty(0, T; H^1(\Omega))^3 \cap L^2(0, T; H^2(\Omega))^3$ for any finite $T < t^*$.

Proof

Step 1: Strict Amplitude Bound. Prove by contradiction: assume there exists $(\boldsymbol{x}_0, t_0) \in (\Omega \setminus \partial\Omega) \times (0, t^*)$ such that $|\boldsymbol{u}'(\boldsymbol{x}_0, t_0)| \geq |\langle \boldsymbol{u} \rangle(\boldsymbol{x}_0, t_0)|$. By Theorem 3.1, $\langle u \rangle(\boldsymbol{x}_0, t_0) \geq c > 0$, so this assumption implies the total velocity $\boldsymbol{u} = \langle \boldsymbol{u} \rangle + \boldsymbol{u}'$ would have a non-positive streamwise component at $(\boldsymbol{x}_0, t_0)$. This violates the maximum principle for smooth Couette flow solutions and physical consistency—within the laminar/pre-singularity regime $t < t^*$, no mathematical or physical mechanism enables disturbances to reverse the direction of positive mean flow. Thus, the strict inequality $|\boldsymbol{u}'| < |\langle \boldsymbol{u} \rangle|$ holds globally on $\Omega \times [0, t^*)$.

Step 2: Regularity of Disturbance. On $[0, t^*)$, the instantaneous velocity $\boldsymbol{u}$ is smooth (local well-posedness of NSE for smooth initial data), so $\boldsymbol{u} \in L^\infty(0, T; H^1(\Omega))^3 \cap L^2(0, T; H^2(\Omega))^3$ for all finite $T < t^*$. The mean velocity $\langle \boldsymbol{u} \rangle$ is also smooth and uniformly bounded in $H^2(\Omega)$ (Theorem 3.2). The disturbance $\boldsymbol{u}' = \boldsymbol{u} - \langle \boldsymbol{u} \rangle$ is the difference of two smooth H^k-regular functions, so it inherits identical regularity in Sobolev spaces. All functions are classical smooth solutions on $[0, t^*)$. By the linearity of Sobolev space norms, we have:

$$\|\boldsymbol{u}'\|_{H^1(\Omega)} \leq \|\boldsymbol{u}\|_{H^1(\Omega)} + \|\langle \boldsymbol{u} \rangle\|_{H^1(\Omega)} \tag{12}$$

$$\|\boldsymbol{u}'\|_{H^2(\Omega)} \leq \|\boldsymbol{u}\|_{H^2(\Omega)} + \|\langle \boldsymbol{u} \rangle\|_{H^2(\Omega)} \tag{13}$$

Based on the velocity decomposition and regularity analysis in Section 3, we further define singularities and derive preliminary inequalities in Section 4 to lay a foundation for the main proof.

4. Preliminaries and Singularity Definitions

4.1. *Energy-Velocity Monotonicity Principle (EVMP)*

In Dou (2025), based on physical intuition and observations, an axiom was proposed. This axiom states: "The velocity of fluid particles monotonically changes with their energy loss during motion, and vice versa."

According to this axiom, the velocity of fluid particles is always determined by the energy loss along the streamlines. For a specific fluid particle, its speed increases as energy is consumed during motion. In the absence of energy loss, the velocity would be zero. For the shear-driven plane Couette flow, the energy loss (or the energy expensed) is equal to the energy dissipation (Dou 2022). Thus, in terms of this axiom, the following Theorem 4.1 can be deduced.

Theorem 4.1 Consider the laminar shear-driven plane Couette flow with no-slip boundary conditions, where the flow field is an incompressible viscous fluid satisfying the unsteady Navier-Stokes equations. For any point $\boldsymbol{x} \in \Omega$ in the flow field, if:

1. The local instantaneous time derivative is zero: $\dfrac{\partial \boldsymbol{u}}{\partial t} = 0$;

2. The local energy dissipation rate is zero: $\mu \|\nabla \boldsymbol{u}(\boldsymbol{x}, t)\|^2 = 0$;

Then it must hold that $|\boldsymbol{u}(\boldsymbol{x}, t)| = 0$.

The proof of the Theorem 4.1 is provided in the Appendix.

doi:10.20944/preprints202603.1511.v2

Implications of Theorem 4.1 At any position in pure shear-driven flows of viscous fluid, zero energy dissipation rate (zero velocity gradient) cannot sustain non-zero velocity.

1. For $\frac{\partial \boldsymbol{u}}{\partial t} = 0$, there are two cases, (a) Steady flow; (b) In unsteady flow, this occurs at the maximum or the minimum of the disturbance velocity.

2. For any point in the flow field, if $\frac{\partial \boldsymbol{u}}{\partial t} = 0$ and $\mu\|\nabla \boldsymbol{u}(\boldsymbol{x},t)\|^2 = 0$, the solution of the Navier-Stokes equations is only $\boldsymbol{u} = 0$. If the velocity is not zero when $\frac{\partial \boldsymbol{u}}{\partial t} = 0$ and $\mu\|\nabla \boldsymbol{u}(\boldsymbol{x},t)\|^2 = 0$, this non-zero velocity does not satisfy the system of the Navier-Stokes equations and is no longer the solution of the Navier-Stokes equations at this time moment. This means that at this while, the position at this point is a physical singularity of the Navier-Stokes equations.

4.2. *Singularity Definitions in Plane Couette Flow*

Combined with the characteristics of shear-driven plane Couette flow, we define two types of singularities related to velocity gradients and velocity discontinuities, which are core concepts for proving the non-existence of global smooth solutions.

Definition 4.1 (Singularity from Zero Velocity Gradient)

In shear-driven plane Couette flow, if there exists a point $\boldsymbol{x}_0 \in \Omega$ and a finite time $t^* > 0$ such that the local velocity gradient of the instantaneous velocity satisfies $\nabla \boldsymbol{u}(\boldsymbol{x}_0, t) \to 0$ as $t \to t^*$, then the point $\boldsymbol{x}_0$ is called a **singularity** of the 3D NSE as $t \to t^*$.

This definition characterizes the physical singularity in shear-driven flows. This singularity definition is tailored to shear-driven plane Couette flow, consistent with the energy gradient theory (Theorem7.3, on page 229 in Dou 2022).

Definition 4.2 (Singularity from Velocity Discontinuity)

In shear-driven plane Couette flow, if there exists a point $\boldsymbol{x}_0 \in \Omega$ and a finite time $t^* > 0$ such that the left limit of the instantaneous velocity at $\boldsymbol{x}_0$ satisfies $\lim_{\boldsymbol{x}\to\boldsymbol{x}_0^-} \boldsymbol{u}(\boldsymbol{x},t) > 0$ and the right limit satisfies $\lim_{\boldsymbol{x}\to\boldsymbol{x}_0^+} \boldsymbol{u}(\boldsymbol{x},t) = 0$ as $t \to t^*$, then the point $\boldsymbol{x}_0$ is called a **singularity** of the 3D NSE as $t \to t^*$ due to velocity discontinuity. This singularity is not velocity blow-up, but loss of smoothness.

This definition characterizes a mathematical singularity, as it satisfies the non-differentiability requirement of mathematical singularities. It can be seen later that in fact, there is a causal relationship between Definition 4.1 and Definition 4.2. The emergence of physical singularities (Definition 4.1) leads to the occurrence of mathematical singularities (Definition 4.2).

4.3. *BKM Criterion*

The Beale-Kato-Majda (BKM) criterion is a classic result for the breakdown of smooth solutions to the 3D NSE, establishing a relationship between solution breakdown and the growth of the vorticity norm (Beale et al. 1984). This criterion was proposed for the Euler equation in Beale et al. (1984). Later, it is extended to the Navier-Stokes equations (Kozono and Taniuchi 2000; Zhao 2017; Gibbon et al. 2018). Vorticity is defined as $\boldsymbol{\omega} = \nabla \times \boldsymbol{u}$, which reflects the rotational characteristics of the fluid.

Lemma 4.1 (BKM Criterion): Let $\boldsymbol{u}(t)$ be a smooth solution of the 3D incompressible NSE on $[0, t^*)$, with the initial vorticity $\boldsymbol{\omega}_0 = \nabla \times \boldsymbol{u}_0 \in L^1(\Omega) \cap L^\infty(\Omega)$. If the solution fails at $t = t^*$ (i.e., its regularity breaks down), then the following integral diverges:

$$\int_0^{t^*} \|\boldsymbol{\omega}(s)\|_{L^\infty(\Omega)} ds = \infty \tag{14}$$

Conversely, if the integral is finite, the solution can be smoothly extended beyond t^*. The BKM criterion applies here since the smooth solution exists on $[0, t^*)$ and the initial vorticity $\boldsymbol{\omega}_0 \in L^1(\Omega) \cap L^\infty(\Omega)$.

For plane Couette flow, vorticity is mainly determined by the velocity gradient in the normal direction, and the growth of the velocity gradient norm leads to the growth of the vorticity norm. Thus, the BKM criterion is an important basis for judging singularity formation in the flow field.

doi:10.20944/preprints202603.1511.v2

5. Singularity Formation and Non-Existence of Global Smooth Solutions

In this section, we will give the main theorem on finite-time singularity formation in shear-driven plane Couette flow. Then, based on previous definitions on singularities and preliminary lemmas, we will prove that the solutions to the Navier-Stokes equations do not exist beyond a finite time t^* for $Re > Re_{cr}$. The solution procedure is outlined in Figure 2.

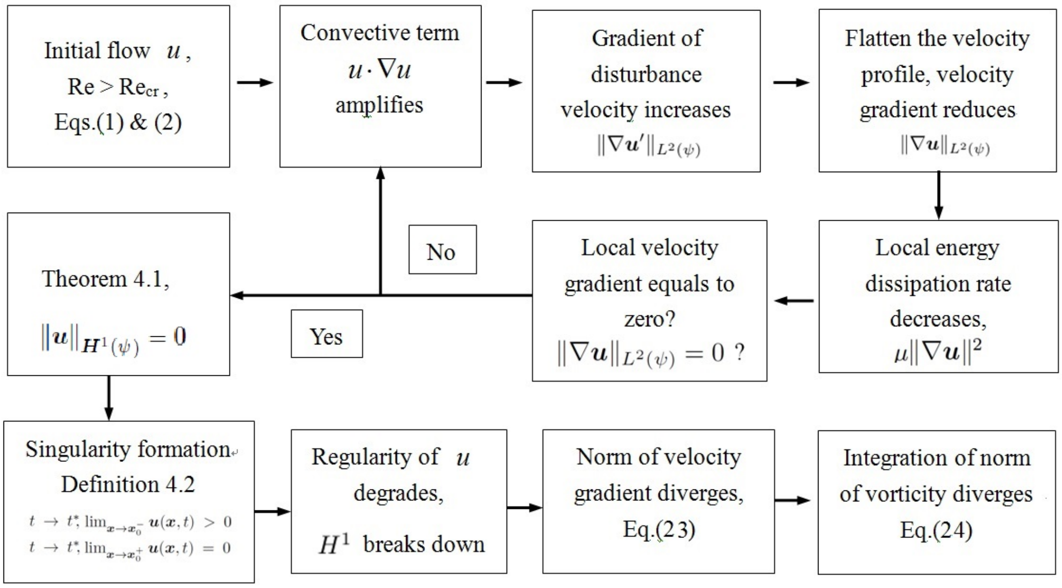

Figure 2. Logical chain for singularity generation and regularity breaking of solutions to the 3D Navier-Stokes equations in plane Couette flow, Sobolev space foundation. The cycle represents the process of the disturbance amplification with the sequential time increments from $t = 0$ to $t = t_n$ at the position x_0.

5.1. Main Theorem on Finite-Time Singularity Formation

Firstly, it is assumed that the disturbance velocity varies periodically in the laminar flow range before singularity formation $[0, t^*)$. Further, it is assumed that the disturbance velocity gradient follows a sine function of the phase angle ωt.

Figure 3 shows various flow variables versus the phase angle ωt of the disturbance at the critical condition of singularity formation. In (a), the mean velocity gradient $\nabla\langle \boldsymbol{u}\rangle$ remains almost constant in a short time window as sequential time increment. In (b), the disturbance velocity gradient $\nabla \boldsymbol{u}'$ varies periodically with the phase angle in this time window. In (c), the instantaneous velocity gradient, $\nabla \boldsymbol{u}$, is the sum of $\nabla\langle \boldsymbol{u}\rangle$ and $\nabla \boldsymbol{u}'$. In (d), it is shown that the instantaneous velocity $\boldsymbol{u}$ varies with the phase angle ωt at the critical condition of singularity formation. The behaviours of various flow variables at the critical condition of singularity will be proven in the following derivations.

In order to reduce the complexity of the main theorem, we first give the Lemma 5.1 to demonstrate how the velocity gradient at the channel centerline gradually reduces to zero during the flow evolution at $Re > Re_{cr}$. It will be seen later that the feature of **velocity gradient tending to zero at channel centerline** characterizes the solution regularity breakdown and the turbulent onset.

Lemma 5.1 (Local Nonlinear Cancellation of Velocity Gradients): For the three-dimensional incompressible Navier-Stokes equations describing the plane Couette flow, assume that:

1. The flow satisfies the governing equations, boundary conditions, and initial laminar linear velocity profile described in Section 2;
2. The Reynolds number exceeds the critical value, i.e., $Re > Re_{cr}$;
3. The disturbance velocity $\boldsymbol{u}'$ is smooth on the time interval $[0, t^*)$.

Then, there exists a finite time T (with $0 < T \leq t^*$) and a non-empty open subset $\psi \in \Omega \setminus \partial\Omega$ in the interior of the flow field, such that as time t approaches T from the left ($t \to T^-$), the disturbance velocity gradient cancels the mean velocity gradient in the $L^2(\psi)$ -norm sense (due to opposite directions). Specifically:

$$\lim_{t\to T} \|\nabla \boldsymbol{u}'(\cdot,t) + \nabla\langle \boldsymbol{u}\rangle(\cdot,t)\|_{L^2(\psi)} = 0, \tag{15}$$

Corollary: From this Lemma and the linearity of the gradient operator, the following equation follows directly:

$$\lim_{t\to T} \|\nabla \boldsymbol{u}(\cdot,t)\|_{L^2(\psi)} = \lim_{t\to T} \|\nabla \boldsymbol{u}'(\cdot,t) + \nabla\langle \boldsymbol{u}\rangle(\cdot,t)\|_{L^2(\psi)} = 0, \tag{16}$$

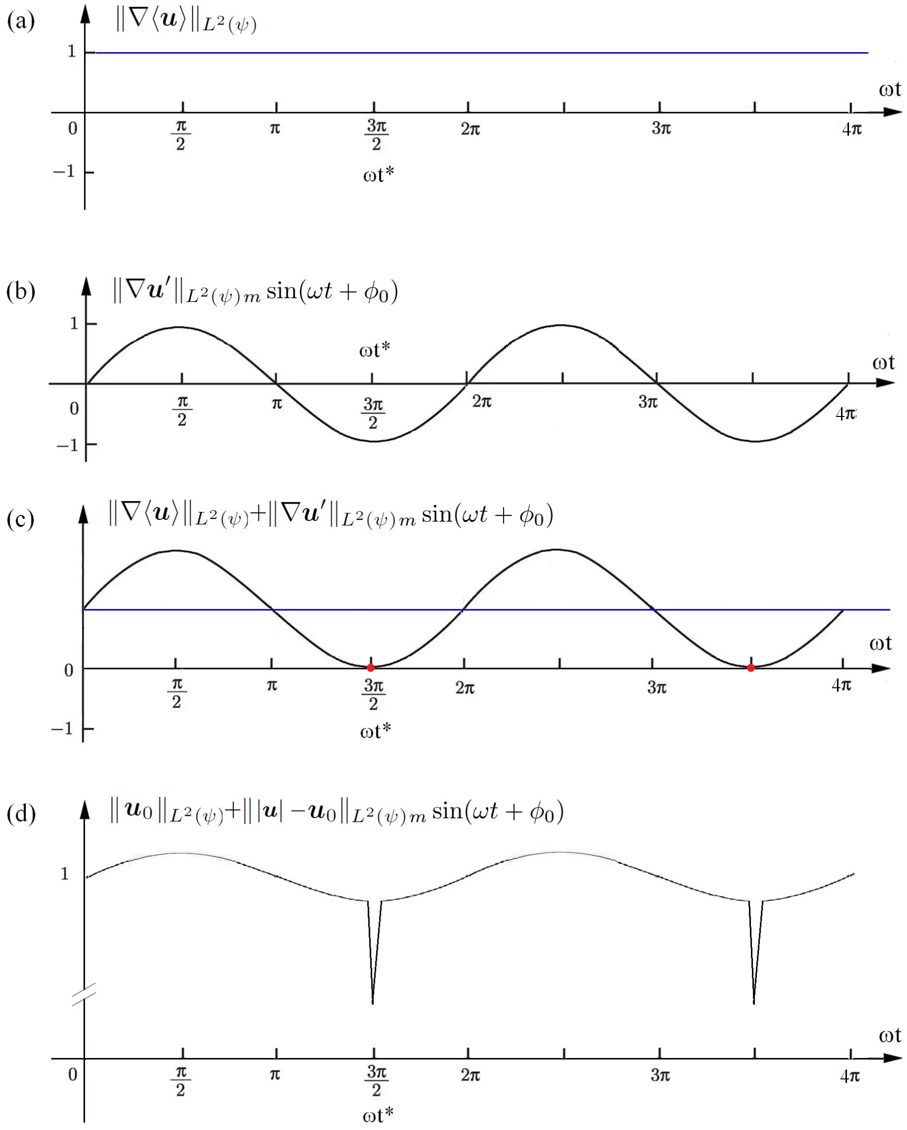

Figure 3. Schematic of appearance of velocity discontinuity (spike) at the position of x_0 and at the phase angle ωt^*. All the variables at the ordinate are normalized, ϕ_0 is the initial phase angle, and the subscript m represents the amplitude. (a) The mean velocity gradient; (b) The disturbance velocity gradient; (c) The instantaneous velocity gradient; (d) The instantaneous velocity. Note: In the evolution of flow from the initial flow state to the formation of velocity discontinuity, we take two periods of phase angle variation near the critical time t^* of singularity at x_0, which is shown in this figure. The phase angle $\omega t^* = 3\pi/2$ in the figure is the first appearance of the velocity discontinuity. For all $0 \le t < t^*$, $\|\nabla \boldsymbol{u}(x_0,t^*)\|_{L^2(\psi)} > 0$; At $t = t^*$, $\|\nabla \boldsymbol{u}(x_0,t^*)\|_{L^2(\psi)} = 0$ for the first time, as accessed by the Theorem 4.1.

Proof

Step 1. Opposite Sign of $\nabla \boldsymbol{u}'$ to $\nabla \langle \boldsymbol{u} \rangle$ in a Half Period.

For $Re > Re_{cr}$, the nonlinear term $(\boldsymbol{u} \cdot \nabla)\boldsymbol{u}$ in the NSE dominates the viscous term $\frac{1}{Re}\Delta \boldsymbol{u}$. The initial linear laminar velocity profile is distorted by the disturbance development. In the instantaneous laminar flow field of the plane Couette flow, the disturbance velocity varies periodically with time, so does the gradient of the disturbance velocity, as shown in Figure 3. Since the variation of the disturbance velocity gradient is pulsating, there is always a half in a period that the disturbance velocity gradient $\nabla \boldsymbol{u}'$ has the opposite sign to the mean velocity gradient $\nabla \langle \boldsymbol{u} \rangle$ at a local point of the flow field. Thus, in this half period, the mean velocity gradient is offset partly by the disturbance velocity gradient. Further, at the phase angle of the maximum amplitude of the disturbance velocity gradient in the half opposite sign period, the norm of the instantaneous velocity gradient is the minimum because the disturbance velocity gradient offsets the mean velocity gradient the most, as $\nabla \boldsymbol{u} = \nabla \langle \boldsymbol{u} \rangle + \nabla \boldsymbol{u}'$. If the disturbance is amplified sufficiently, the $\nabla \langle \boldsymbol{u} \rangle$ will be cancelled by $\nabla \boldsymbol{u}'$ at this phase angle at this local point, and $\nabla \boldsymbol{u} \to 0$.

Step 2. Increase of $\nabla \boldsymbol{u}'$ due to Nonlinear Amplification and the Velocity Profile Flattened at Centerline.

According to the velocity decomposition (Equation (7)), the nonlinear term can be rewritten as:

$$(\boldsymbol{u} \cdot \nabla)\boldsymbol{u} = (\langle \boldsymbol{u} \rangle \cdot \nabla)\langle \boldsymbol{u} \rangle + (\langle \boldsymbol{u} \rangle \cdot \nabla)\boldsymbol{u}' + (\boldsymbol{u}' \cdot \nabla)\langle \boldsymbol{u} \rangle + (\boldsymbol{u}' \cdot \nabla)\boldsymbol{u}' \tag{17}$$

The last three terms are nonlinear interaction terms between the mean velocity and the disturbance velocity, which are the sources of disturbance amplification. The growth of $\nabla \boldsymbol{u}'$ distorts the original linear mean velocity profile $\langle \boldsymbol{u} \rangle$, rendering the mean velocity gradient $\nabla \langle \boldsymbol{u} \rangle$ a non-constant function of space and time. For $Re > Re_{cr}$, as time evolves, these nonlinear terms continuously amplify the disturbance velocity $\boldsymbol{u}'$, and the disturbance velocity gradient $\nabla \boldsymbol{u}'$ grows accordingly. Thus, the total integration of the energy dissipation rate in the whole domain grows with time, and the input power by the upper plate must be increased. Owing to the moving velocity of the upper plate is fixed, the shear force (hence the velocity gradient) acting on the plate must be increased. This leads to the decrease of the magnitude of the velocity gradient toward the centerline from the wall. Therefore, the velocity profile at the centerline is flattened.

The second and third terms in the right hand side, $(\langle \boldsymbol{u} \rangle \cdot \nabla)\boldsymbol{u}' + (\boldsymbol{u}' \cdot \nabla)\langle \boldsymbol{u} \rangle$, are the main terms playing important roles in amplifying the disturbance. In the second term, $(\langle \boldsymbol{u} \rangle \cdot \nabla)\boldsymbol{u}'$, **the mean velocity $\langle \boldsymbol{u} \rangle$ is proportional to the disturbance velocity gradient $\nabla \boldsymbol{u}'$**, which induces exponential increase of the disturbance at the sequential time increments (Schmid and Henningson 2001). Thus, in the evolution of the velocity profile, the second term $(\langle \boldsymbol{u} \rangle \cdot \nabla)\boldsymbol{u}'$ is the dominating term in amplifying the disturbance. In the core zone of the channel, the disturbance is amplified more than those near the walls, then, the velocity gradient is reduced gradually. As such, the energy dissipation rate is reduced, which gives a **positive feedback** to further result in disturbance increase due to reduced viscous damping. Gradually, **the velocity profile at the centerline is flattened by the disturbance**, and thus the role of the third term, $(\boldsymbol{u}' \cdot \nabla)\langle \boldsymbol{u} \rangle$, becomes small gradually. Further, because the mean velocity gradient becomes small at the centerline, the first cancelation of $\|\nabla \langle \boldsymbol{u} \rangle\|_{L^2(\psi)}$ by $\|\nabla \boldsymbol{u}'\|_{L^2(\psi)}$ at a local subset should occur there (Figure 1(b)).

Step 3. Cancelation of $\nabla \langle \boldsymbol{u} \rangle$ by $\nabla \boldsymbol{u}'$ at the Channel Centerline.

The instantaneous velocity gradient is the sum of the mean velocity gradient and the disturbance velocity gradient: $\nabla \boldsymbol{u} = \nabla \langle \boldsymbol{u} \rangle + \nabla \boldsymbol{u}'$. With the disturbance evolution continuously, it is inevitably that the mean velocity gradient $\nabla \langle \boldsymbol{u} \rangle$ is cancelled eventually by the disturbance velocity gradient $\nabla \boldsymbol{u}'$ at a local open subset $\psi \in \Omega \setminus \partial\Omega$ for $Re > Re_{cr}$.

Therefore, there exists a local open subset $\psi \in \Omega \setminus \partial\Omega$ and a time sequence $t_n \to t^*$ such that the local $L^2(\psi)$ norm of the disturbance velocity gradient satisfies:

$$\|\nabla \boldsymbol{u}\|_{L^2(\psi)} = \|\nabla \langle \boldsymbol{u} \rangle + \nabla \boldsymbol{u}'\|_{L^2(\psi)} = 0, \quad t = t_n \tag{18}$$

That is, the local velocity gradient of the instantaneous velocity vanishes in the subset ψ as $t \to t^*$. As $t \to t^*$,

$$\|\nabla \boldsymbol{u}'\|_{L^2(\psi)} = \|\nabla \langle \boldsymbol{u} \rangle\|_{L^2(\psi)}, \quad t = t_n \tag{19}$$

but the phase is opposite.

In the ψ region, the saturation amplitude of the disturbance velocity gradient $\nabla u'$ is determined by the mean velocity gradient $\nabla \langle \boldsymbol{u} \rangle$, and the phase relationship is locked in anti-phase. As discussed previously, the ψ region is located at the centerline due to the balance of the energy transfer in the whole domain.

With Lemma 5.1 established, we now proceed to prove the main theorem (Theorem 5.1) by demonstrating that the local cancellation of the velocity gradient inevitably leads to the finite-time singularity.

Theorem 5.1 (Locally blow-up of the norm of the velocity gradient): For 3D plane Couette flow governed by the Navier-Stokes equations Eqs.(1)-(2) with the initial laminar linear velocity profile (Equation (5)), when the Reynolds number exceeds the critical value $Re > Re_{cr}$, there exists a finite time $t^* > 0$ such that singularities form in the flow field as $t \to t^*$. As $t \to t^*$, firstly, there is a local open subset where the local velocity gradient tends to zero, which leads to the velocity becomes zero locally, as defined in Definition 4.1. Then, the regularity of the 3D NSE breaks down due to velocity discontinuity caused by instability, which is characterized by the divergence of the local Sobolev space norms of the velocity gradient. Specifically, for any integer $k \geq 1$, the local H^k norm of the velocity gradient $\|\nabla \boldsymbol{u}\|_{H^k(\psi)}$ (where ψ is a local open subset containing the singularity) tends to infinity, which satisfies the singularity definition (Definition 4.2) and leads to regularity breakdown of the 3D NSE. Thus, the global regularity of the solution fails to hold when $t > t^*$. Consequently, the 3D Navier-Stokes equations for plane Couette flow have **no global smooth solutions** at condition of $Re > Re_{cr}$.

5.2. Proof of the Main Theorem

We prove the main theorem (Theorem 5.1) step-by-step, combining velocity decomposition, Sobolev space analysis, the EVMP, and the BKM criterion, and verifying singularity formation in accordance with Definitions 4.1 and 4.2.

Step 1: Vanishing of the Instantaneous Velocity Gradient Locally

At $Re > Re_{cr}$, the nonlinear amplification of disturbances results in flattening of the velocity profile at centerline and finally leads to the vanishing of the instantaneous velocity gradient locally.

According to Lemma 5.1, when $Re > Re_{cr}$, there exists a local region ψ and a time sequence $t_n \to t^{*-}$ such that the $\nabla \langle \boldsymbol{u} \rangle$ is cancelled by $\nabla \boldsymbol{u}'$ locally (as indicated in Figure 3 (a), (b) and (c)),

$$\|\nabla \boldsymbol{u}\|_{L^2(\psi)} = \|\nabla \langle \boldsymbol{u} \rangle + \nabla \boldsymbol{u}'\|_{L^2(\psi)} = 0 \tag{20}$$

This occurs at the phase angle ωt^* shown in Figure 3(c), where the instantaneous velocity gradient $\nabla \boldsymbol{u} = \nabla \langle \boldsymbol{u} \rangle + \nabla \boldsymbol{u}'$ locally vanishes as $t \to t^*$.

Step 2: Vanishing of the Local Velocity via the EVMP

The velocity gradient $\|\nabla \boldsymbol{u}\|_{L^2(\psi)} = 0$ implies that:

$$\mu \|\nabla \boldsymbol{u}\|^2_{L^2(\psi)} = 0, \tag{21}$$

this means that there is no energy dissipation at this local point.

From the Theorem 4.1, for the instantaneous velocity $\boldsymbol{u}$ in the local subset $\psi \subset \Omega$, we have:

$$\|\boldsymbol{u}\|_{L^2(\psi)} = 0 \tag{22}$$

Since $\boldsymbol{u}$ is continuous (as a smooth solution of the NSE on $[0, t^*)$), Equation (22) implies that $\boldsymbol{u}(\boldsymbol{x}, t) = 0$ for all $\boldsymbol{x} \in \psi$ as $t \to t^*$. Thus, the local gradient of the instantaneous velocity at any point $\boldsymbol{x}_0 \in \psi$ tends to zero: $\nabla \boldsymbol{u}(\boldsymbol{x}_0, t) \to 0$ as $t \to t^*$.

Step 3: Singularity Formation from Zero Velocity Gradient

By Theorem 4.1, the mean velocity in the interior of the domain $\Omega \setminus \partial\Omega$ has a positive lower bound: $\langle u\rangle(\boldsymbol{x}) \geq c > 0$ for all $\boldsymbol{x} \in \Omega \setminus \partial\Omega$. The local subset ψ is an interior subset of Ω (hence $\psi \subset \Omega \setminus \partial\Omega$), so the mean velocity at $\boldsymbol{x}_0 \in \psi$ satisfies $\langle \boldsymbol{u}\rangle(\boldsymbol{x}_0, t) > 0$ for all $t > 0$.

However, from Step 2, the instantaneous velocity at $\boldsymbol{x}_0 \in \psi$ satisfies $\boldsymbol{u}(\boldsymbol{x}_0, t) \to 0$ as $t \to t^*$. This leads to a contradiction: the instantaneous velocity is the sum of a positive mean velocity and a disturbance velocity, yet the instantaneous velocity vanishes at the interior point $\boldsymbol{x}_0$. By Definition 4.1 (Singularity from Zero Velocity Gradient), the point $\boldsymbol{x}_0$ is a singularity of the 3D NSE as $t \to t^*$.

Step 4: Singularity Formation from Velocity Discontinuity

For the singularity point $\boldsymbol{x}_0 \in \psi$, the instantaneous velocity at $\boldsymbol{x}_0$ tends to zero as $t \to t^*$, i.e., $\lim_{\boldsymbol{x}\to\boldsymbol{x}_0} \boldsymbol{u}(\boldsymbol{x}, t) = 0$. In the neighborhood of $\boldsymbol{x}_0$, take a point $\boldsymbol{x}_1 \in \Omega \setminus \psi$ close to $\boldsymbol{x}_0$: the mean velocity at $\boldsymbol{x}_1$ remains positive ($\langle \boldsymbol{u}\rangle(\boldsymbol{x}_1, t) > 0$), and the disturbance velocity is smaller than the mean velocity ($|\boldsymbol{u}'(\boldsymbol{x}_1, t)| < |\langle \boldsymbol{u}\rangle(\boldsymbol{x}_1, t)|$), so the instantaneous velocity at $\boldsymbol{x}_1$ satisfies $\boldsymbol{u}(\boldsymbol{x}_1, t) > 0$.

Thus, the left limit (or upper limit) of the instantaneous velocity at $\boldsymbol{x}_0$ is positive ($\lim_{\boldsymbol{x}\to\boldsymbol{x}_0^-} \boldsymbol{u}(\boldsymbol{x}, t) > 0$), and the right limit (or lower limit) is zero ($\lim_{\boldsymbol{x}\to\boldsymbol{x}_0^+} \boldsymbol{u}(\boldsymbol{x}, t) = 0$). By Definition 4.2 (Singularity from Velocity Discontinuity), the point $\boldsymbol{x}_0$ is a singularity of the 3D NSE as $t \to t^*$ due to velocity discontinuity.

In the real status of the plane Couette flow and the Taylor-Couette flow, a vertical velocity drop (from $\boldsymbol{u} > 0$ to $\boldsymbol{u} = 0$) is not observed, but a **"negative velocity spike" is produced owing to effects of fluid inertia and viscosity**. This is the correlation and difference between the "velocity discontinuity" in mathematics and the "negative velocity spike" observed in experiments and numerical simulations. The instantaneous velocity $\boldsymbol{u}$ varying with ωt in the given short time window at the critical condition of singularity formation is shown in Figure 3(d) by present mathematical analysis. It can be observed from Figure 3(d) that "negative velocity spike" is produced in the instantaneous velocity $\boldsymbol{u}$ at ωt^* as $t \to t^*$. This phenomenon has been found in experiments and numerical simulations (Kitoh et al. 2005; Zhou et al. 2025). Generally, the amplitude of the spike is a fraction of the incoming velocity about $(0.3 - 0.7)|\boldsymbol{u}|$, as shown at the phase angle ωt^* in Figure 3(d). In the Figure 24 in Kitoh et al. (2005), it is clearly showed by experiments that how a negative velocity spike is produced at the channel centerline of plane Couette flow and how it develops into multiple spikes as the time evolution, which characterizes the onset of turbulence.

Step 5: Breakdown of Regularity and Divergence of Integration of the Vorticity Norm

A smooth solution of the 3D NSE requires that the velocity and all its derivatives are bounded in Sobolev spaces for all $t > 0$. However, at the singularity point x_0, the instantaneous velocity gradient vanishes as $t \to t^*$, and the velocity is discontinuous at x_0. To ensure flow field continuity and the incompressibility condition Equation (1), the velocity gradient in the neighborhood of $\boldsymbol{x}_0$ must grow rapidly (instability setting in), leading to the divergence of the local Sobolev space norms of the velocity gradient as $t \to t^*$:

$$\|\nabla \boldsymbol{u}\|_{H^k(\psi)} \to \infty, \quad \forall k \geq 1,\ t \to t^* \tag{23}$$

Vorticity $\boldsymbol{\omega} = \nabla \times \boldsymbol{u}$ is a linear combination of the velocity gradient components, so the local vorticity norm also tends to infinity: $\|\boldsymbol{\omega}\|_{L^\infty(\psi)} \to \infty$ as $t \to t^*$.

Strictly, the velocity gradient is bounded by the vorticity (Beale et al. 1984; Bledsoe, 2025, page 17),

$$\|\nabla \boldsymbol{u}\|_{L^p(\Omega)} \leq k_p \|\boldsymbol{\omega}\|_{L^p(\Omega)}, \qquad (1 < p < \infty)$$

By the BKM criterion (Lemma 4.1), the integral of the vorticity L^∞ norm over the time interval $[0, t^*)$ diverges:

$$\int_0^{t^*} \|\boldsymbol{\omega}(s)\|_{L^\infty(\Omega)} ds \geq \int_0^{t^*} \|\boldsymbol{\omega}(s)\|_{L^\infty(\psi)} ds = \infty \tag{24}$$

doi:10.20944/preprints202603.1511.v2

This implies that the smooth solution of the 3D NSE cannot be smoothly extended beyond the singularity time t^*, and the Sobolev space regularity of the solution breaks down as $t \to t^*$. Specifically, the velocity gradient $\nabla \boldsymbol{u}$ becomes locally unbounded, with its $L^\infty(0,T;H^k(\Omega))$ norm diverging for any $k \geq 1$ and any $T > t^*$, while the velocity $\boldsymbol{u}$ itself remains finite and uniformly bounded in $L^\infty(0,T;L^2(\Omega))$. Therefore, the loss of global regularity is caused by the blow-up of the velocity gradient, not by the blow-up of the velocity magnitude.

Step 6: Conclusion on the Non-Existence of Global Smooth Solutions

Since there exists a finite time $t^* > 0$ such that the smooth solution of the 3D NSE for plane Couette flow does not exist at $t = t^*$ (singularities form and regularity breaks down), the 3D NSE has no smooth solution on $[0,\infty)$. Thus, the 3D Navier-Stokes equations for plane Couette flow have no global smooth solutions when $Re > Re_{cr}$.

5.3. *Velocity Field $\boldsymbol{u}$ and Velocity Gradient $\nabla\boldsymbol{u}$ at Regularity Breakdown (as $t \to t^*$)*

In previous sub-section 5.2, we proved that global smooth solutions to the 3D NSE do not exist for plane Couette flow as $t \to t^*$. This is due to the regularity breakdown of solutions caused by the vanishing of the norm of the velocity gradient and the subsequent divergence of the norm of the velocity gradient locally at $Re > Re_{cr}$. In the following, the behaviours of the velocity and its gradient at regularity breakdown are summarized.

As $t \to t^*$, the cancellation between the disturbance velocity gradient and the mean velocity gradient near the channel centerline triggers a local singularity, leading to a complete collapse of flow regularity. The Sobolev space regularity of the velocity and the velocity gradient undergoes a drastic drop, with specific properties detailed below:

1. Velocity Field $\boldsymbol{u}$ at Regularity Breakdown

- Mathematical Characterization: $\boldsymbol{u} \in L^\infty(0,t^*;H^0(\Omega))^3 = L^\infty(0,t^*;L^2(\Omega))^3$, with loss of H^1 and higher-order regularity.
- Mathematical Interpretation: The velocity field only retains its own L^2 square-integrability, remaining uniformly bounded in time with no global velocity blow-up (pointwise finite $\boldsymbol{u}$). However, it no longer satisfies the H^1 regularity requirement of square-integrable first-order weak derivatives, completing the core degradation from $H^1 \to H^0(L^2)$.
- Physical Interpretation: The velocity field is globally continuous with finite kinetic energy, but its local smoothness is completely lost, entering the critical state of laminar-turbulent transition.

2. Velocity Gradient $\nabla\boldsymbol{u}$ at Regularity Breakdown

- Mathematical Characterization: $\nabla\boldsymbol{u} \notin H^0(\Omega)^3 = L^2(\Omega)^3$, with regularity dropping from H^0 to the negative-order Sobolev space $H^{-s}(\Omega)^3$ ($s \geq 1$), accompanied by blow-up of local H^k norms for $k \geq 1$.
- Mathematical Interpretation: The velocity gradient completely loses L^2 integrability and cannot be characterized by non-negative order Sobolev spaces; it can only be described in weak form via negative-order dual spaces. This is not a simple order reduction, but a full collapse of non-negative order regularity and local norm blow-up.
- Physical Interpretation: The vanishing of the local velocity gradient induces singularity and discontinuity in the gradient field, invalidating the viscous dissipation effect. This satisfies the singularity criterion of the Beale-Kato-Majda (BKM) theorem, directly leading to the non-existence of global smooth solutions to the 3D NSE.

6. Discussions and Conclusions

In this paper, we conduct a strict mathematical analysis of the 3D plane Couette flow based on the Sobolev space theory in functional analysis, and prove the non-existence of global smooth solutions to the 3D Navier-Stokes equations for $Re > Re_{cr}$. The discussions and the main conclusions of this study are as follows:

1. We establish the mathematical model of 3D plane Couette flow, define the smooth solutions of the NSE in Sobolev space, and prove the uniqueness of the velocity decomposition of the instantaneous

doi:10.20944/preprints202603.1511.v2

velocity into the mean velocity and the disturbance velocity. We also verify the boundedness of the mean velocity and its gradient, as well as the Sobolev regularity of the disturbance velocity, which lays the foundation for the subsequent singularity analysis.

2. For $Re > Re_{cr}$, the nonlinear term in the NSE dominates the viscous term, leading to the continuous amplification of the disturbance velocity and the distortion of the mean velocity profile. In the local region of the flow field (core region near the centerline of the flow channel), the disturbance is mostly amplified due to effect of less viscosity damping and the velocity profile is flattened gradually with time evolution. As such, **the flow at the centerline has the minimum norm of velocity gradient over the domain**. At this condition, the disturbance velocity gradient with the opposite sign to the mean velocity gradient at a specific phase angle cancels the mean velocity gradient, resulting in the vanishing of the local instantaneous velocity gradient.

3. Based on the Energy-Velocity Monotonicity Principle (EVMP), Theorem 4.1, the vanishing of the local velocity gradient implies the vanishing of the local instantaneous velocity at the interior point of the local sub-domain, which contradicts the value of the instantaneous velocity in the neighbour point upstream, thus forming a singularity from the zero velocity gradient as in Definition 4.1. Consequently, the velocity discontinuity (caused by instability) at the singularity point forms a mathematical singularity as in Definition 4.2, which further confirms the singularity formation in the flow field.

4. Combined with the BKM criterion, the singularity formation leads to the rapid growth of the velocity gradient norm and the vorticity norm in the neighborhood of the singularity point, making the local Sobolev norm of the velocity gradient tend to infinity and the integral of the vorticity L^{∞} norm diverge. This results in the breakdown of regularity of the 3D NSE, and the smooth solution cannot be extended to the infinite time, thus proving the non-existence of global smooth solutions. As we can see in this study that the singularity occurred in the shear-driven plane Couette flow is **not the blow-up of the velocity, but the regularity breakdown of solutions**.

5. This study defines two types of singularities (zero velocity gradient and velocity discontinuity), and it can be observed in the proof that **both singularities appear consecutively**. The velocity discontinuity is a direct consequence of the zero velocity gradient. Firstly, in step 3, based on the EVMP, the velocity gradient being zero leads to the conclusion that the velocity is zero; then, considering the velocity of adjacent points being positive, this "velocity being zero" at current point leads to the "zero velocity gradient singularity." Secondly, in step 4, based on the left limit of the singularity being positive and the right limit being zero, the velocity discontinuity singularity is obtained.

6. The energy gradient theory (Axiom 5.4 on page 146 in Dou 2022) shows that a non-zero velocity of fluid particle must be compensated by an energy loss, while zero energy loss is not able to sustain a non-zero velocity. Therefore, for shear-driven flow, when the energy dissipation rate becomes zero (the energy loss along the streamline is zero for shear-driven flow), the velocity must be zero. This is in agreement with that implied by the EVMP. Following this way, for plane Couette flow, the core mechanism underlying singularity formation is that **the zero energy dissipation rate at the channel centerline fails to dampen disturbances, leading to unbounded disturbance amplification (Constantin and Foias 1988)**.

7. Physical Implications of Theorem 4.1 on Discovering Singularity. For the shear-driven laminar plane Couette flow, the flow in the whole domain is driven by the work input from the upper moving plate. The shear force is transmitted continuously to the bottom plate by the upper plate. Along the y direction, all the fluid particles consume energy by energy dissipation $\mu\|\nabla \boldsymbol{u}(\boldsymbol{x},t)\|^2$. All the velocity values on the velocity profile are the solutions of the Navier-Stokes equations.

In disturbed laminar flows of plane Couette flow, the velocity profile at the centerline is flattened gradually with the disturbance development. When the velocity gradient at the channel centerline $\|\nabla \boldsymbol{u}(\boldsymbol{x},t)\| = 0$ under the condition of $\frac{\partial \boldsymbol{u}}{\partial t} = 0$, the energy dissipation becomes zero locally, but the velocity is a non-zero value. **This non-zero velocity at the centerline is no longer the solution of the Navier-Stokes equations at this time moment, because it does not satisfy the Navier-Stokes equations and the boundary conditions**. For this point with zero velocity gradient, the solution of the

Navier-Stokes equations is only a zero velocity with the boundary condition constraints. This means that at this while, the position at the centerline is a physical singularity of the Navier-Stokes equations.

However, this mentioned singularity is never reported in the literature and in the community except in the publications by the author and collaborators.

8. The velocity discontinuities predicted by Sobolev space theory manifest as spikes in the instantaneous velocity distribution in experimental studies and numerical simulations. This is due to effects of the fluid viscosity and fluid inertia; negative velocity spikes are formed, instead of sharp vertical jump. These spikes have been found in pipe and plane Poiseuille flows (Nishioka et al. 1975; Han et al. 2000), wake flows (Tiwari et al. 2019; Niu et al. 2024) and boundary layer flows (Rist and Fasel 1995; Kachanov 1994). For shear-driven flows, these spikes have been found in plane Couette flow (Kitoh et al. 2005), and Taylor-Couette flows (Zhou et al. 2025). Gibbon (2010) conjectured that spikes might be the real singularity, and the present study confirms his idea about the singularity. As such, **the velocity discontinuity predicted by the Sobolev space theory is in agreement with the "negative velocity spike" obtained in experiments and numerical simulations**.

9. Non-existence of global smooth solutions to the 3D NSE for plane Couette flow above the critical Reynolds number is proved, bridging the gap between the energy gradient theory (Dou 2022) and the rigorous PDE analysis. The key findings confirm that **zero velocity gradient at the channel centerline acts as the trigger for singularity formation, which destroys the regularity of the 3D NSE and rules out global smooth solutions**. The results align with numerical observations and experimental evidence of turbulence onset during laminar-turbulent transition in plane Couette flow (Dou and Khoo 2012; Lee 1990; Kitoh et al. 2005; Cherubini and De Palma 2015; Couliou and Monchaux 2015), providing a mathematical foundation for understanding turbulence onset in shear-driven flows.

10. This paper provides a strict mathematical theoretical proof for the experimental and numerical simulation results of Dou and Khoo (2010, 2011, 2012) about the turbulence generation condition in 3D plane Couette flow, and also gives a new result for the regularity problem of the 3D Navier-Stokes equations for shear-driven flows. The research method based on Sobolev space analysis and the EVMP can be extended to the regularity analysis of other shear-driven flows, which provides a mathematical framework for the study of laminar-turbulent transition and singularity formation in viscous incompressible flow.

Funding: No external funding was received for this study.

Institutional Review Board Statement: This research work is performed by the author independently.

Data Availability Statement: The data supporting the findings of this study are available from the corresponding author upon reasonable request.

Acknowledgments: Thanks are due to the Computing Research Center of Zhejiang Sci-Tech University for computational support.

Conflicts of Interest: The authors have no conflicts of interest or competing interests to disclose.

Appendix A. Theorem 4.1 Proof (Functional Analysis & PDE)

Appendix A.1. Theorem Statement

Consider laminar shear-driven plane Couette flow equipped with no-slip Dirichlet boundary conditions. For any spatial point $\boldsymbol{x} \in \Omega$ and time $t > 0$,

$$\frac{\partial \boldsymbol{u}}{\partial t} = 0 \quad \text{and} \quad \mu \|\nabla \boldsymbol{u}(\boldsymbol{x}, t)\|^2 = 0 \implies |\boldsymbol{u}(\boldsymbol{x}, t)| = 0. \tag{A1}$$

Mathematical Interpretation: Within the weak solution framework for the incompressible Navier–Stokes equations governing shear-driven Couette flow, simultaneous vanishing of the temporal velocity derivative and the viscous dissipation functional in the Sobolev space uniquely enforces the trivial velocity field at every interior point .

Appendix A.2. Mathematical Preliminaries (Functional Analysis & PDE Theory)

1. Governing Equations and Functional Setting

Let $\Omega \subset \mathbb{R}^3$ denote a bounded, connected Lipschitz domain corresponding to the flow domain of plane Couette flow. The unsteady, incompressible Navier–Stokes system with zero body force is well-posed in the function space class:

$$\begin{cases} \dfrac{\partial \boldsymbol{u}}{\partial t} + (\boldsymbol{u} \cdot \nabla)\boldsymbol{u} = -\dfrac{1}{\rho}\nabla p + \nu \Delta \boldsymbol{u}, \\ \nabla \cdot \boldsymbol{u} = 0, \end{cases} \tag{A2}$$

where $\boldsymbol{u} \in L^2(0, T; \boldsymbol{H}^1(\Omega)) \cap L^\infty(0, T; \boldsymbol{L}^2(\Omega))$ is the velocity field, p denotes the pressure field, ρ is the constant fluid density, μ is the dynamic viscosity, and $\nu = \mu/\rho > 0$ denotes the kinematic viscosity. The operators ∇, $\nabla\cdot$, and Δ represent the gradient, divergence, and vector Laplacian, respectively.

2. Boundary Conditions

The plane Couette configuration adopts no-slip Dirichlet boundary conditions on the upper and lower solid walls, with $y \in [0, h]$ defining the wall-normal coordinate:

$$\boldsymbol{u}(0,0,0) = (0,0,0), \quad \boldsymbol{u}(0,h,0) = (U_1,0,0). \tag{A3}$$

This boundary trace constraint fully characterizes the boundary-driven nature of the Couette flow system and restricts the admissible solution manifold within $\boldsymbol{H}^1(\Omega)$.

3. Fundamental Hypotheses

The theorem assumes two pointwise conditions valid at a fixed $(\boldsymbol{x}, t)$ with $\boldsymbol{x} \in \Omega, t > 0$:

Temporal stationarity: $\partial_t \boldsymbol{u}(\boldsymbol{x}, t) = \boldsymbol{0}$, meaning the velocity field attains a temporal extremum at the given point and time.

Zero viscous dissipation: Define the dissipation functional $\mathcal{D}[\boldsymbol{u}] = \mu|\nabla \boldsymbol{u}|^2$. The condition $\mathcal{D}[\boldsymbol{u}] = 0$ is equivalent to $\nabla \boldsymbol{u}(\boldsymbol{x}, t) = \boldsymbol{0}$ due to the non-negative definiteness of the squared gradient norm.

Appendix A.3. Rigorous Proof via PDE and Functional Analysis

Step 1: Local Constant Field Deduction from Zero Gradient

For a vector-valued Sobolev function $\boldsymbol{u} \in \boldsymbol{H}^1(\Omega)$, the squared gradient norm is defined as $|\nabla \boldsymbol{u}|^2 = \sum i, j = 1^3(\partial j u_i)^2$. Since the sum of non-negative real terms vanishes if and only if every term vanishes individually:

$$\|\nabla \boldsymbol{u}\|^2 = 0 \iff \partial_j u_i = 0, \quad \forall\, i, j \in \{1, 2, 3\}. \tag{A4}$$

On any connected open subdomain $\psi(\boldsymbol{x}) \subset \Omega$, a function with vanishing first-order weak derivatives is locally constant. Therefore, there exists a time-dependent constant vector $\boldsymbol{M}(t) \in \mathbb{R}^3$ such that:

$$\boldsymbol{u}(\boldsymbol{\xi}, t) \equiv \boldsymbol{M}(t), \quad \forall\, \boldsymbol{\xi} \in \psi(\boldsymbol{x}). \tag{A5}$$

Step 2: Compatibility with Incompressibility Constraint

Substitute the locally constant velocity field Equation (A5) into the divergence-free incompressibility condition. All spatial derivatives of constant vectors are identically zero, so:

$$\nabla \cdot \boldsymbol{M}(t) = 0. \tag{A6}$$

The incompressibility constraint is trivially satisfied, yielding no contradiction at this step.

Step 3: Simplification of Stationary Momentum Equation

Under the temporal stationarity condition $\partial_t \boldsymbol{u} = \boldsymbol{0}$, the unsteady Navier–Stokes system reduces to a stationary PDE. Substitute $\boldsymbol{u} \equiv \boldsymbol{M}(t)$ into the momentum equation:

$$(\boldsymbol{M} \cdot \nabla)\boldsymbol{M} = -\frac{1}{\rho}\nabla p + \nu \Delta \boldsymbol{M}. \tag{A7}$$

For constant vector fields, both the nonlinear convection operator and the Laplace operator produce zero output:

$$(\boldsymbol{M} \cdot \nabla)\boldsymbol{M} = \mathbf{0}, \quad \Delta \boldsymbol{M} = \mathbf{0}. \tag{A8}$$

Substituting Equation (A8) into Equation (A7) yields a vanishing pressure gradient:

$$\nabla p(\boldsymbol{\xi}, t) \equiv \mathbf{0}, \quad \forall \boldsymbol{\xi} \in \psi(\boldsymbol{x}). \tag{A9}$$

The pressure field is therefore locally constant within the neighborhood $\psi(\boldsymbol{x})$.

Step 4: Variational Energy Identity Analysis

Define the standard $\boldsymbol{L}^2$ kinetic energy inner product $\mathcal{E}(\boldsymbol{u}, \boldsymbol{v}) = \int_\Omega \boldsymbol{u} \cdot \boldsymbol{v}\, d\boldsymbol{x}$. Testing the momentum equation against $\boldsymbol{u}$ over the local subdomain $\psi(\boldsymbol{x})$ gives the variational energy identity:

$$\int_\psi \boldsymbol{u} \cdot \partial_t \boldsymbol{u}\, d\boldsymbol{x} + \int_\psi \boldsymbol{u} \cdot (\boldsymbol{u} \cdot \nabla)\boldsymbol{u}\, d\boldsymbol{x} = -\frac{1}{\rho}\int_\psi \boldsymbol{u} \cdot \nabla p\, d\boldsymbol{x} + \nu \int_\psi \boldsymbol{u} \cdot \Delta \boldsymbol{u}\, d\boldsymbol{x}. \tag{A10}$$

Applying the two core hypotheses: $\partial_t \boldsymbol{u} = \mathbf{0}$ eliminates the transient term, and $\nabla \boldsymbol{u} = \mathbf{0}$ restricts $\boldsymbol{u}$ to a constant field $\boldsymbol{M}$. All nonlinear and pressure gradient integrals vanish identically.

For the viscous term, apply Green's first identity for vector-valued functions:

$$\nu \int_\psi \boldsymbol{u} \cdot \Delta \boldsymbol{u}\, d\boldsymbol{x} = -\nu \int_\psi \|\nabla \boldsymbol{u}\|^2 d\boldsymbol{x} + \nu \int_{\partial\psi} \boldsymbol{u}(\nabla \boldsymbol{u} \cdot \boldsymbol{n}) dS. \tag{A11}$$

Under $\nabla \boldsymbol{u} = \mathbf{0}$, both the volume dissipation integral and the boundary integral vanish. The entire variational identity degenerates to $0 = 0$, which is a trivial equality and provides no local interior constraint. Thus, global boundary compatibility must be invoked for solvability.

Step 5: Boundary-Driven Solvability Constraint

Plane Couette flow is a strictly boundary-forced shear flow, whose solution manifold in $\boldsymbol{H}^1(\Omega)$ is uniquely determined by the Dirichlet boundary traces in Equation (A3). For Newtonian viscous fluids, the viscous stress tensor is defined as:

$$\tau_{ij} = \mu(\partial_j u_i + \partial_i u_j), \quad 1 \le i, j \le 3. \tag{A12}$$

The zero-gradient condition $\nabla \boldsymbol{u} = \mathbf{0}$ implies all velocity derivatives vanish, leading to identically zero viscous stress:

$$\partial_j u_i \equiv 0 \implies \tau_{ij} \equiv 0, \quad \forall i, j. \tag{A13}$$

The streamwise stationary momentum balance reduces to the shear stress equilibrium relation:

$$0 = -\partial_x p + \partial_y \tau_{xy}. \tag{A14}$$

Local trivialization of pressure gradient and shear stress yields $0 = 0$, but crucially, a non-zero constant velocity field $\boldsymbol{M} \neq \mathbf{0}$ cannot belong to the solution set of the Couette boundary-value problem. The boundary trace condition enforces a strictly y-dependent velocity profile, which excludes constant interior solutions.

Step 6: Proof by Contradiction and Uniqueness

Assume for contradiction that the theorem hypotheses hold while the conclusion fails. That is, there exists

$$\partial_t \boldsymbol{u}\big|_\psi = \mathbf{0}, \quad \|\nabla \boldsymbol{u}\|^2_{L^2(\psi)} = 0, \quad \|\boldsymbol{u}\|_{\boldsymbol{H}^1(\psi)} = |\boldsymbol{M}| > 0. \tag{A15}$$

This assumption implies $\boldsymbol{u} \equiv \boldsymbol{M} \neq \boldsymbol{0}$ is a nontrivial constant weak solution to the stationary Navier–Stokes equations on $\psi(\boldsymbol{x})$. However, the weak solution uniqueness of the Dirichlet boundary-value problem for Couette flow prohibits nontrivial constant interior solutions (Galdi 2011): the admissible solution manifold consists solely of y-varying shear profiles compatible with the wall velocity boundary conditions.

The hypothesized nontrivial constant solution violates global boundary compatibility and is not an admissible weak solution in $\boldsymbol{H}^1(\Omega)$. This contradiction eliminates all non-zero velocity candidates. Consequently, the only mathematically admissible solution is the trivial field:

$$\boldsymbol{M} = \boldsymbol{0} \implies \boldsymbol{u}(\boldsymbol{x}, t) = \boldsymbol{0}. \tag{A16}$$

Therefore,

$$\boxed{\partial_t \boldsymbol{u}\big|_{\psi(\boldsymbol{x})} = \boldsymbol{0} \quad \wedge \quad \mu\|\nabla \boldsymbol{u}\|^2_{\boldsymbol{L}^2(\psi(\boldsymbol{x}))} = 0 \implies \|\boldsymbol{u}\|_{\boldsymbol{H}^1(\psi(\boldsymbol{x}))} = 0} \tag{A17}$$

or

$$\boxed{\frac{\partial \boldsymbol{u}}{\partial t} = 0 \quad \wedge \quad \mu\|\nabla \boldsymbol{u}(\boldsymbol{x}, t)\|^2 = 0 \implies |\boldsymbol{u}(\boldsymbol{x}, t)| = 0} \tag{A18}$$

Based on Sobolev space operator analysis, variational energy functional identities, and weak solution uniqueness of the stationary incompressible Navier–Stokes system (Galdi 2011), the logical implication of Theorem 4.1 is rigorously established. Thus, the Theorem 4.1 is proved.

Funding: No external funding was received for this study.

Data Availability Statement: The data supporting the findings of this study are available from the corresponding author upon reasonable request.

Acknowledgments: Thanks are due to the Computing Research Center of Zhejiang Sci-Tech University for computational support.

Conflicts of Interest: The authors have no conflicts of interest or competing interests to disclose.

References

Adams, R. A., Fournier, J.J.F. 2003. Sobolev Spaces, 2nd Ed., Academic Press, New York.

Beale, J.T., Kato, T., Majda, A. 1984. Remarks on the breakdown of smooth solutions for the 3-D Euler equations, Commun. Math. Phys., 94(1), 61-66.

Bledsoe, B. 2025. A constructive framework for global regularity in the 3D Navier-Stokes equations, Preprint, Available at SSRN: http://dx.doi.org/10.2139/ssrn.5575415

Brezis, H. 2011. Functional Analysis, Sobolev Spaces and Partial Differential Equations, Springer, New York.

Buckmaster, T., Vicol, V. 2019. Nonuniqueness of weak solutions to the Navier-Stokes equation, Annals of Mathematics, 189, 101-144.

Caffarelli, L., Kohn, R., Nirenberg, L. 1982. Partial regularity of suitable weak solutions of the Navier-Stokes equations. Communications on Pure and Applied Mathematics, 35(6), 771-831.

Cherubini, S., De Palma, P. 2015. Minimal-energy perturbations rapidly approaching the edge state in Couette flow, J. Fluid Mech., 764, 572–598.

Coiculescu, M.P., Palasek, S. 2025. Non-uniqueness of smooth solutions of the Navier–Stokes equations from critical data. Inventiones Mathematicae, Online first. https://doi.org/10.1007/s00222-025-01396-z.

Couliou, M., Monchaux, R. 2015. Large-scale flows in transitional plane Couette flow: a key ingredient of the spot growth mechanism, Phys. Fluids, 27, 034101.

Constantin, P., Foias, C. 1988. Navier-Stokes Equations, University of Chicago Press, Chicago.

Doering, C. R. 2009. The 3D Navier-Stokes problem, Annu. Rev. Fluid Mech., 41, 109-128.

Dou, H.-S. 2022. Origin of Turbulence-Energy Gradient Theory, Springer, Singapore. https://link.springer.com/book/10.1007/978-981-19-0087-7

Dou, H.-S. 2025. Singular solution of the Navier-Stokes equation for plane Poiseuille flow, Physics of Fluids, 37, 084131. https://doi.org/10.1063/5.0284009

Dou, H. -S., Khoo, B.C. 2010. Criteria of turbulent transition in parallel flows, Modern Physics Letters B, 24(13), 1437-1440.

Dou, H.S., Khoo, B.C. 2011. Investigation of Turbulent transition in plane Couette flows Using Energy Gradient Method, Advances in Appl. Math. and Mech., 3(2), 165-180.

Dou, H.-S., Khoo, B. C. 2012. Direct numerical simulation of turbulent transition for plane Couette flows using full Navier-Stokes equations, in Proceedings of 50th AIAA Aerospace Sciences Meeting Including the New Horizons Forum and Aerospace Exposition, 9-12 January 2012, Nashville, Tennessee, USA.

Fefferman, C. L. 2006. Existence and smoothness of the Navier-Stokes equation. In: The Millennium Prize Problems, Carlson, J., Jaffe, A., Wiles, A., Editors, American Mathematical Society, pp. 57-67.

Foias, C., Manley, O., Rosa, R., Temam, R. 2004. Navier-Stokes Equations and Turbulence, Cambridge University Press, Cambridge, UK.

Galdi, G. P. 2011. An Introduction to the Second Edition Mathematical Theory of the Navier-Stokes Equations (2nd edition), Springer, New York.

Gibbon, J. D. 2010. Regularity and singularity in solutions of the three-dimensional Navier-Stokes equations, Proc. Royal Soc A, 466, 2587-2604.

Gibbon, J. D., Gupta, A., Pal, N., Pandit, R. 2018. The role of BKM-type theorems in 3D Euler, Navier-Stokes and Cahn–Hilliard–Navier–Stokes analysis, Physica D: Nonlinear Phenomena, 376–377, 60-68.

Han, G., Tumin, A., Wygnanski, I. 2000. Laminar-turbulent transition in Poiseuille pipe flow subjected to periodic perturbation emanating from the wall, Part 2. Late stage of transition, J. Fluid Mech., 419, 1-27.

Hof, B., Juel, A., Mullin, T. 2003. Scaling of the turbulence transition threshold in a pipe, Phys. Rev. Lett., 91, 244502.

Kachanov, Y. S. 1994. Physical mechanisms of laminar-boundary-layer transition, Annu. Rev. Fluid Mech., 26, 411–482.

Khan, H. H., Anwer, S. F., Hasan, N., Sanghi, S. 2021. Laminar to turbulent transition in a finite length square duct subjected to inlet disturbance, Physics of Fluids 33, 065128. https://doi.org/10.1063/5.0048876.

Kitoh, O., Nakabyashi, K., Nishimura, F. 2005. Experimental study on mean velocity and turbulence characteristics of plane Couette flow: low-Reynolds-number effects and large longitudinal vortical structure, J. Fluid Mech., 539, 199–227. doi:10.1017/S0022112005005641

Kozono, H., Taniuchi, Y. 2000. Bilinear estimates in BMO and the Navier-Stokes equations. Mathematische Zeitschrift, 235(1), 173-194.

Lee, M. J. 1990. Direct numerical simulation of turbulent plane Couette flow, Annual Reaearch Brief of Center for Turbulence Reaearch, Stanford University, pp. 133-143.

Leray, J. 1934. Sur le mouvement d'un liquide visqueux emplissent l'espace, Acta Math., 63, 193-248.

Niu, L., Dou, H.-S., Zhou, C., Xu, W. 2024. Turbulence generation in the transitional wake flow behind a sphere, Physics of Fluids, 36, 034127. https://doi.org/10.1063/5.0199349

Rist, U., Fasel, H. 1995. Direct numerical simulation of controlled transition in a flat-plate boundary layer, J Fluid Mech., 298, 211–248.

Robinson J. C. 2020. The Navier–Stokes regularity problem. Phil. Trans. R. Soc. A, 378, 20190526. http://dx.doi.org/10.1098/rsta.2019.0526

Robinson, J. C. 2021. Using periodic boundary conditions to approximate the Navier-Stokes equations on R 3 and the transfer of regularity, Nonlinearity 34 (2021), no. 11, 7683–7704.

Scheffer, V. 1976. Turbulence and Hausdorff dimension, In Turbulence and the Navier–Stokes equations, Lecture Notes in Math., 565, Springer, Berlin, 94-112.

Schmid, P. J., Henningson, D. S. 2001. Stability and transition in shear flows. Springer, New York.

Serrin, J. 1962. On the interior regularity of weak solutions of the Navier-Stokes equations, Arch. Rational Mech. Anal., 9(1), 187-195.

Tao, T. 2016. Finite time blowup for an averaged three-dimensional Navier-Stokes equation, Journal of the American Mathematical Society, 29 (3), 601-674.

Taylor, M. E. 2011. Partial Differential Equations I: Basic Theory, Second Ed., Springer, New York.

Tiwari, S. S., Bale, S., Patwardhan, A. W., Nandakumar, K., Joshi, J. B. 2019. Insights into the physics of dominating frequency modes for flow past a stationary sphere: Direct numerical simulations, Physics of Fluids, 31, 045108.

Zhao, J. 2017. BKM's criterion for the 3D nematic liquid crystal flows via two velocity components and molecular orientations, Mathematical Methods in the Applied Sciences, 40(4), 871-882.

Zhou, C., Dou, H.-S., Niu, L., Xu, W. 2025a. Inverse energy cascade in turbulent Taylor–Couette flows, Phys. Fluids, 37, 014110. https://doi.org/10.1063/5.0250908